Proposal for the BGOegg Phase-II Experiment — A study of the η' mass inside a nucleus —

N. Muramatsu and M. Miyabe

Research Center for Electron Photon Science, Tohoku University

1-2-1 Mikamine, Taihaku, Sendai, Miyagi 982-0826, Japan

e-mail : mura@lns.tohoku.ac.jp, miyabe@lns.tohoku.ac.jp

Jan 14, 2022

Contents

Abstract

We propose second-phase programs of the BGOegg experiment particularly to promote a search for the medium modification of the η' spectral function. Such an experiment is achievable by performing a direct measurement of the η' mass through the $\gamma\gamma$ decay mode inside a nucleus. Only the BGOegg experiment currently makes this measurement possible with the world's highest resolution. We plan to improve the signal sensitivity by reducing backgrounds with the upgrade of detector setup and increasing the data statistics with a high-intensity photon beam and a copper nucleus target. We request a half-year beamtime for the first physics run of the Phase-II experiment with a $0.5X_0$ copper target in FY2023. We aim to confirm the Phase-I result by analyzing the new data. We also need additional beamtimes to collect test-data with a 0.1 X_0 copper target and reference data with a LH_2 target.

1 Introduction

The mass of a hadron composed of u, d, and s quarks cannot be described by a sum of their current-quark masses, generated by interactions with the Higgs field. For example, such a sum accounts for only about 1% of the nucleon mass. Thus, a dynamical mechanism of hadron-mass generation proposed by Nambu is widely believed in modern physics. In this mechanism, the quantum-mechanical vacuum changes its ground-state properties by the spontaneous breaking of chiral symmetry as the universe evolves from a high-temperature and high-density plasma of massless quarks. This phenomenon is called chiral phase transition, and its order parameter is a vacuum expectation value of quark condensates. Under the spontaneous breaking of chiral symmetry, a constituent quark mass is given to a quark through interactions with the quark condensates.

In recent years, the η' meson has attracted much attention for studying the origin of a hadron mass. The main component of η' is a singlet state in the flavor $SU(3)$ nonet of pseudoscalar mesons. Its mass (958 MeV/c^2) is extraordinarily heavier than the other octet members, corresponding to Nambu-Goldstone bosons. Historically, the η'-meson mass has been explained by the $U_A(1)$ quantum anomaly [1, 2]. However, it is also known that the η' and other mesons like π, σ, and η must degenerate when the chiral symmetry is restored [3]. This means that the mass generation in η' is closely related with both the $U_A(1)$ quantum anomaly and the spontaneous breaking of chiral symmetry. In addition, it has been theoretically found that the spontaneous breaking of chiral symmetry can be caused if the $U_A(1)$ quantum anomaly is strong enough [4].

Efforts to prove the above mass-generation mechanism have been actively attempted in the research field of hadron physics. Partial restoration of the chiral symmetry is expected to take place inside a nucleus, which has an ultra-high density of about 10^{14} g/cm^3, as a precursor phenomenon of the chiral phase transition. So far, several theoretical models have calculated the amount of η'-mass reduction at the normal nuclear density. A calculation based on the Nambu-Jona-Lasinio (NJL) model constructs a Lagrangian with four- and six-fermion terms, which are responsible to the spontaneous breaking of chiral symmetry and the $U_A(1)$ quantum anomaly, respectively. It predicts an η'-mass reduction of 150 MeV/c^2 [5]. In contrast, a calculation based on the linear sigma model adopts a Lagrangian constructed for hadron-level interactions with a σ meson, resulting in a mass reduction of 80 MeV/c^2 [6]. As another prediction, the quark-meson coupling (QMC) model has calculated a 40-MeV/c^2 reduction by using a bag model with a mean filed of σ mesons [7].

From the experimental side, smaller amounts of the η'-mass reduction, which do not exceed

50 MeV/c^2, have been indirectly suggested by the $\eta' N$ scattering length measured at COSY-11 [8] and the results of a nuclear transparency ratio and differential cross sections by the CBELSA/TAPS Collaboration [9, 10, 11, 12, 13]. Recently, the η-PRiME/Super-FRS Collaboration searched for η' bound nuclei, which may be observed if a large mass reduction happens inside a nucleus. They carried out a missing mass spectroscopy in the $^{12}C(p, d)$ reaction, and observed no signals over a background distribution [14, 15]. Therefore, they have concluded that a large mass reduction like the NJL calculation is unfavored.

2 Phase-I results of the BGOegg experiment

Studying the η' meson properties in nuclei must be a clue to clarify the roles and relationship of the spontaneous breaking of chiral symmetry and the $U_A(1)$ quantum anomaly in the mass generation and hadron structure. Both of them should be properly taken into account at the Lagrangians of effective hadron models. The BGOegg experiment, running at SPring-8 LEPS2 beamline, has searched for η'-mass reduction signals in a Carbon nucleus by two complementary methods: One is a missing mass spectroscopy to observe η' bound nuclei in the $^{12}C(\gamma, p)$ reaction [16], and the other is a lineshape analysis for the η' mass spectrum based on the $\gamma\gamma$ invariant mass measurement [17].

Firstly, we have searched for the η' bound nuclei by measuring the momentum of an extremely forward proton through its time-of-flight for a distance of 12.5 m from a Carbon target to a wall of resistive plate chambers (RPC). The RPC wall covers a polar angle range less than 6.8 degrees with a time resolution of 60–90 ps. An excitation energy distribution, corresponding to the missing mass spectrum of the $^{12}C(\gamma, p)X$ reaction, was plotted to examine bound signals below the production threshold of the η' meson. Because there remain a lot of backgrounds, the BGOegg experiment has, for the first time, required the simultaneous detection of nuclear absorption signals from the bound η' mesons ($\eta' N \to \eta N$, followed by $\eta \to \gamma\gamma$) at the BGOegg calorimeter.

Figure 1 shows a scatter plot of the excitation energy and the Lab-frame polar angle of an η meson before (black dots) and after (blue circles) requiring kinematical conditions to increase the signal-to-noise ratio. In the kinematical conditions, back-to-back pairs of an η meson and a slow proton (p_s) were selected to enhance a fraction of the nuclear absorption signals, while the forward production of η or p_s was not allowed to remove backgrounds due to the η or $\eta\pi$ photoproduction with the secondary interactions of primary products, generating a p_s. Finally, no events were observed in the predetermined signal region, indicated by a shaded area. We obtained an upper limit for the production of η' bound nuclei with η-p_s pairs to be

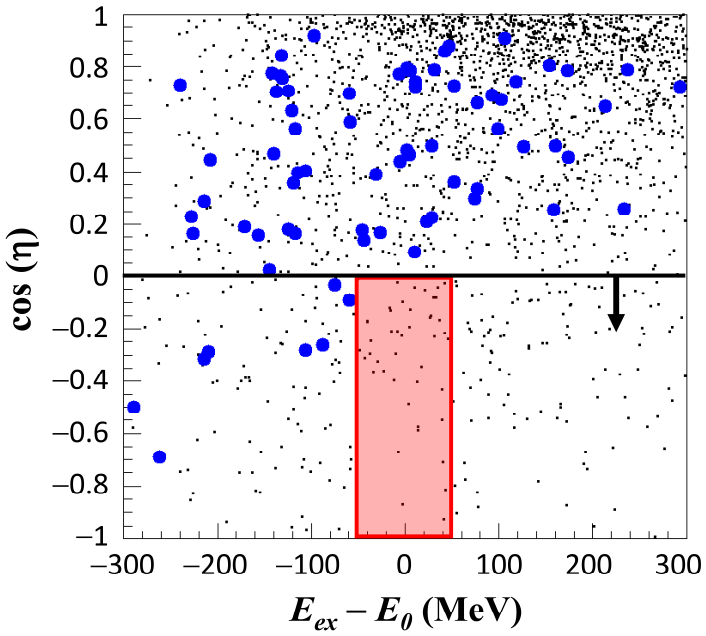

Figure 1: Two-dimensional plot of the η polar angle $\cos(\eta)$ versus the excitation energy $E_{ex} - E_0$ for signal samples of the η' bound nuclei search. The kinematical region of $\cos(\eta) < 0$ was selected to reduce backgrounds. The red shaded area indicates the signal search region.

2.2 nb/sr (90% confidence level) at the opening angles $cos(\eta p_s) < -0.9$. We compared this upper limit with a theoretical calculation using distorted wave impulse approximation (DWIA) for the optical potential $V_0 = -100$ and -20 MeV [18]. For the comparison, we normalized the theoretical calculation by using the quasi-free η' photoproduction process. This normalization was essential to remove ambiguities in the DWIA calculation. As a result, we concluded that a branching fraction of the $\eta' N \to \eta N$ process is constrained to 24% or less for $V_0 = -100$ MeV, indicating that such a large potential is not favored.

In the second method to study the η' mass in nuclei, we focused on the $\eta' \to \gamma\gamma$ decay, whose branching fraction is 2.2%. Direct measurement of an η' mass spectrum is possible by reconstructing the $\gamma\gamma$ invariant mass using the BGOegg calorimeter. If the η'-mass reduction exists at the nuclear density, a component decaying inside a nucleus may be observed at the lower mass side of a quasi-free η' peak. In order to increase the fraction of $\gamma\gamma$ decays inside a nucleus, we selected η' mesons whose momentum was lower than 1 GeV/c. This selection boundary was decided in a simulation study to maximize the signal siginificance. In a lineshape analysis for the measured mass spectrum, even small reduction by several tens of MeV is detectable by recognizing a spectral change at the lower tail of a quasi-free η' peak. The

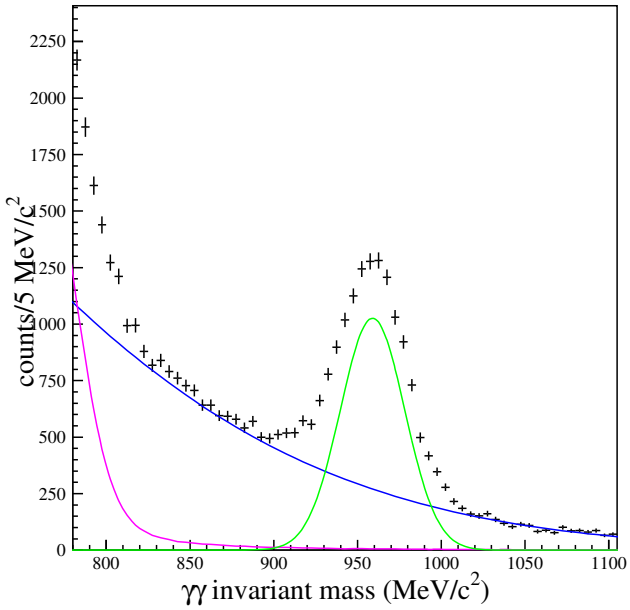

Figure 2: A $\gamma\gamma$ invariant mass distribution for the sample where the momentum of a $\gamma\gamma$ system is lower than 1 GeV/c. Background functions for ω (purple curve), multi-meson (blue curve), and quasi-free η' (green curve) photoproduction processes are fitted to the data collected with a carbon target.

BGOegg experiment has an advantage in such an analysis thanks to the world's best energy resolution of the large solid-angle electromagnetic calorimeter in the energy region below 1 GeV.

Figure 2 shows a $\gamma\gamma$ invariant mass distribution for the low-momentum sample with tight selection of two nuetral clusters at the BGOegg calorimeter. As shown by the fitted functions, there are background components coming from (1) ω photoproduction, followed by the $\omega \to 3\gamma$ decay, (2) smooth and wide-range backgrounds due to multi-π^0 or $\pi^0\eta$ photoproduction, and (3) quasi-free η' photoproduction where the η' meson decays into $\gamma\gamma$ outside a nucleus. The processes (1) and (2) become backgrounds due to undetected γ's escaping into the BGOegg forward acceptance hole. After careful validity checks, the components (1), (2), and (3) were described by a realistic Monte Carlo simulation spectrum, a free-parameter function of $\exp(p_0 + p_1 x + p_2 x^2 + p_3 x^3)$, and a Gaussian function with a fixed mass resolution depending on the η' momentum, respectively.

An excess of event entries over the sum of background functions was examined by fitting them without using the mass range of 870–930 MeV/c^2. We found a statistical significance of the excess to be 3.6σ in the omitted range. This significance was also confirmed by a χ^2

difference test without omitting a mass range for signals. In this test, we compared two fits; One uses only background functions, and the other additionally adopts a signal function, which is simulated with various strengths of the η'-mass reduction. A favored range of the mass reduction was estimated to be approximately 40–70 MeV/c^2. In contrast, reference samples made from the carbon-target data in the $\gamma\gamma$ momentum range above 1 GeV/c and the liquid-hydrogen-target data in the range below 1 GeV/c show statistical significances less than 1σ in the χ^2 difference test. We are now performing further confirmation analyses using existing additional data that have a comparable statistics.

3 Concept of the BGOegg Phase-II experiment

As described in the previous sections, various experimental results indicate the η' optical potential or the η' mass reduction is not very large as -100 MeV. We apparently need to conduct a high-statistics experiment to confirm the BGOegg Phase-I result on the lineshape analysis of an η' mass spectrum. Therefore, we plan to concentrate on the experimental procedure to measure a $\gamma\gamma$ invariant mass distribution by using the BGOegg calorimeter. This procedure is currently only a way to directly reveal the nature of the η' meson inside a nucleus. We set a goal so that an enough signal sensitivity should be achieved over the fluctuation of backgrounds. For this purpose, we upgrade the BGOegg experimental setup as described below.

1. A nuclear target will be replaced from a 20-mm thick carbon block to a copper plate. The radius of a copper nucleus is 1.8 times larger than that of a carbon nucleus, so that a rate of in-medium η'-meson decays is increased. In addition, the target thickness will be increased from 0.1 to 0.5 radiation lengths, corresponding to the copper-plate thickness of 7 mm. A weight per the unit area becomes 1.8 times heavier for the new copper target than that for the carbon target used in the Phase-I experiment. This allows us to collect high statistics data in the Phase-II experiment. Even though the target weight is increased, the actual thickness of the copper target is still thinner, resulting in less ambiguity of reaction vertices. Since the η' mass resolution is determined not only by the energy resolution of a calorimeter but also by the angular accuracy of reconstructed γ's, it will be improved to about 60% of the Phase-I resolution. A test experiment with one-week data taking by using a copper target shows an η' mass resolution of 13 MeV/c^2 in the $\gamma\gamma$ decay mode.

2. As recognized in the BGOegg Phase-I experiment, a majority of widely distributed backgrounds come from multiple π^0 photoproduction. It was not fully removed because some

of final state γ's escaped from the acceptance hole of the BGOegg calorimeter, existing in the polar angles less than 24 degrees. Thus, we cover this forward region by another electromagnetic calorimeter, as described in the next section. A plastic-scintillator wall is also under development for charge identification of forward particles, detected at the new calorimeter. These detector upgrade will reduce the multi-meson backgrounds by an order of magnitudes. In addition, we are considering to expand forward acceptance of the BGOegg calorimeter by adding new BGO crystals. A gap between the current BGOegg calorimeter and the new forward calorimeter will be removed by this expansion, resulting in a higher rejection power for multi-meson backgrounds.

3. An intensity of the photon beam available at the LEPS2 beamline will be increased by introducing pulsed lasers instead of conventional CW lasers. The pulsed laser newly developed by Spectronix Corp. can emit ultraviolet (or deep-ultraviolet) light at a timing synchronized with an electron bunch in the storage ring. All the available laser power is efficiently usable for the production of high energy photons via Compton scattering at the laser focus point. We intend to operate two pulsed lasers simultaneously for the purpose to double the photon beam intensity.

Following the above basic concepts of experimental upgrades, we plan to prepare a new setup of the BGOegg Phase-II experiment as described in the next section. We discuss a signal sesitivity estimation in the next-to-next section.

4 Experimental setup

The BGOegg experiment is carried out at the LEPS2 beamline of SPring-8 [19]. Figure 3 shows an overview of the LEPS2 facility. This facility was constructed as the second beamline of laser Compton scattering at SPring-8 [20], and the first beam was observed in 2013 [21]. It uses one of 30-m long straight sections, which are located only at four places of the storage ring. Thanks to a good electron-beam divergence at the long straight section, a photon beam spread is well limited and we have been able to construct large detector systems in a dedicated experimental building that is about 130 m away from the Compton scattering point. The BGOegg calorimeter and associated detectors are assembled in the upstream part of this building (LEPS2 experimental building).

At the LEPS2 beamline, a photon beam is produced by injecting laser light with the wavelength of 355 nm into the storage ring of 8-GeV electrons. The maximum energy of the photon beam reaches 2.4 GeV. Individual photon energy is measured by the tagger in the range above

1.3 GeV with an energy resolution of 12 MeV. The tagger detects recoil electrons, which lose a part of the energy by laser Compton scattering and leave the electron beam orbit at the bending magnet of the storage ring. The measured momentum of a recoil electron is converted to the photon beam energy by the 4-momentum conservation in Compton scattering. The tagger also counts the reaction rate of Compton scattering to measure a photon beam intensity. We have achieved the maximum tagger rate of $\sim 3 \times 10^6$ s^{-1} by injecting three to four lasers simultaneously. Recently we have introduced a pulsed laser whose output can be adjusted at the timing synchronized with electron beam bunches [22]. A photon beam intensity of 1–3 $\times 10^6$ s^{-1} is being available with the injection of only a pulsed laser depending on the output power, frequency, and timing structure. We are planning to install another pulsed laser and aiming a total intensity of 3–6 $\times 10^6$ s^{-1}.

In the BGOegg Phase-I experiment, we constructed a large-acceptance electromagnetic calorimeter covering a polar angle range of 24 to 144 degrees. We assembled 1320 $Bi_4Ge_3O_{12}$ (BGO) crystals in an egg-shape ("BGOegg" calorimeter), as shown in Fig. 4. Each crystal has a depth of 20 radiation lengths with an inner-side cross section of about 20×20 mm^2. There are no support materials between the crystals. The energy resolution for 1-GeV γ-rays is 1.3% [23].

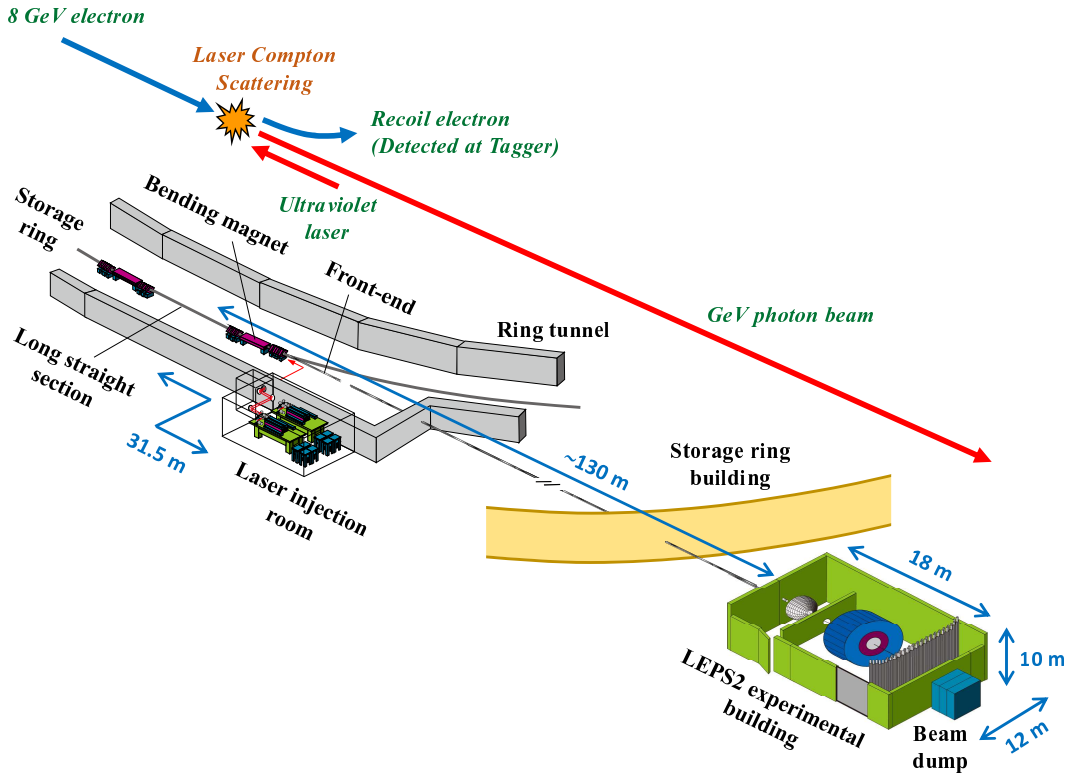

Figure 3: A conceptual overview of the LEPS2 beamline.

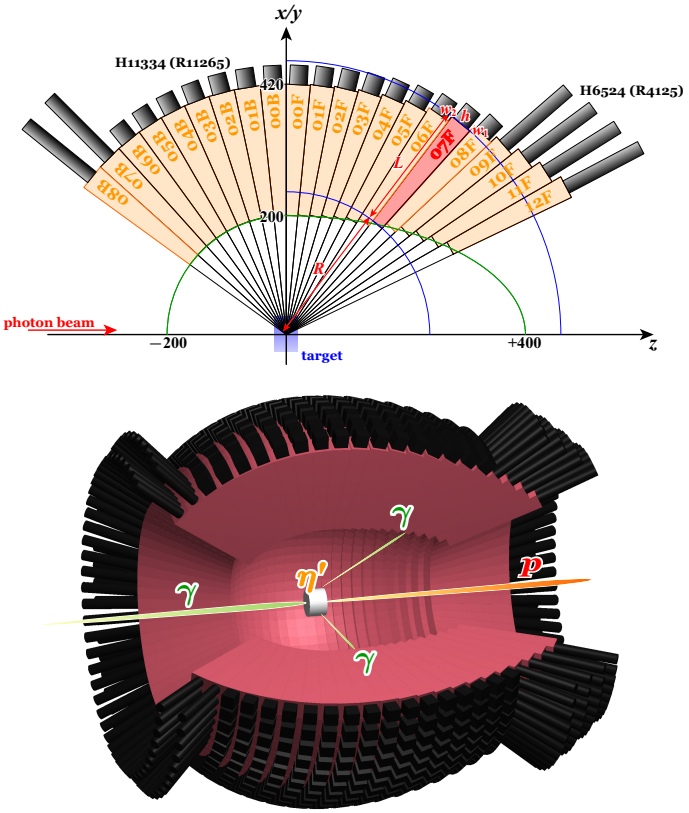

Figure 4: Cross-sectional (upper panel) and schematic (lower panel) views of the BGOegg calorimeter. The centers of the crystal front faces are placed on a prolate spheroid and a sphere for the forward and backward hemispheres, respectively.

The energy resolution and fine segmentation of the BGOegg calorimeter provide the world's best mass resolution for neutral mesons like π^0, η, η', etc. We have additionally installed a cylindrical drift chamber and hodoscopes into the inner volume of the BGOegg calorimeter so that charged and neutral particles can be distinguished from each other for hits in the BGOegg calorimeter. The BGOegg Phase-I experiment has obtained excellent physics results using the high performance detectors [16, 17, 24].

Geometrical acceptance of the BGOegg calorimeter is missing in the foraward region below 24 degrees. In the Phase-I experiment, a planar drift chamber and resistive plate chambers (RPCs) are placed to cover this region on the downstream of the BGOegg calorimeter. The forward acceptance hole is compensated by detecting charged particles with them. In this setup, the η' mesic nuclei search was conducted by measuring the momentum of a charged particle in the extremely forward angles. However, the forward region is still insensitive to γ's from meson decays. We largely loose the acceptance to detect multi-meson photoproduction

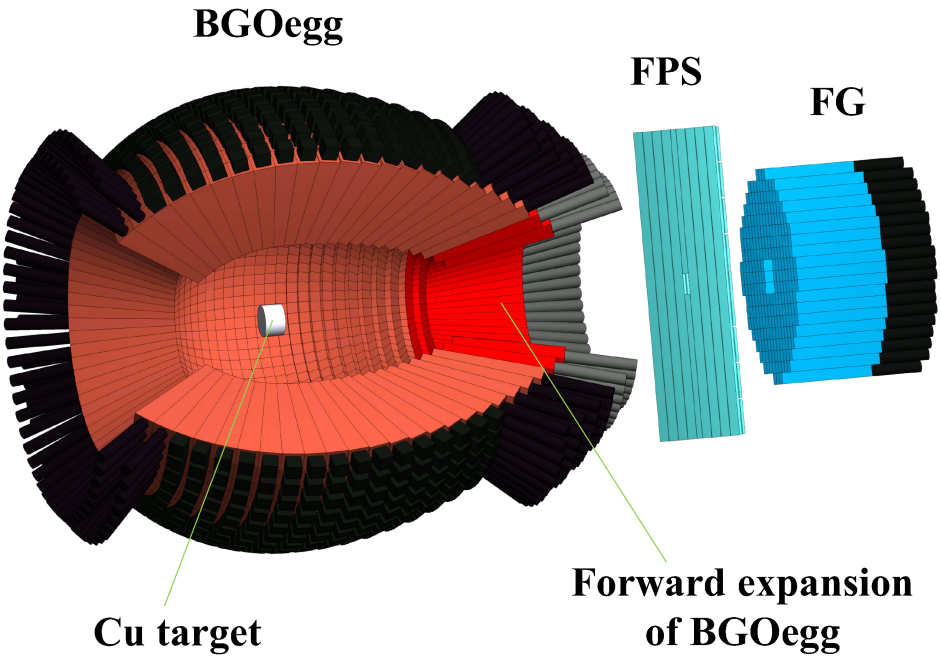

Figure 5: A planned detector setup in the BGOegg Phase-II experiment.

reactions whose final state includes many γ's. This problem is more remarkable in the region of $E_\gamma \sim 2$ GeV or more because such reactions become dominant.

In the BGOegg Phase-II experiment, we are thus preparing another γ-ray detector used at forward angles ("Foward Gamma" or "FG"). Figure 5 shows a planned experimental setup, where the FG is placed on the most downstream. We already developed the FG in past experiments and the acceptance for neutral particles can be recovered by adopting this detector in addition to the BGOegg calorimeter. The FG consists of 252 $PbWO_4$ (PWO) crystals, whose individual size is $22 \times 22 \times 180$ mm^3. After assembling the PWO crystals, the total width and height of the sensitive region both reach 418 mm at the upstream surface. In case that the FG is installed at 700 mm downstream from the target, it will cover 3–16 degrees at forward angles. We also install a wall of newly developed charged-particle identification counters (called "Forward Plastic Scintillators" or "FPS") in front of the FG. The FPS consists of two layers, where the direction of long plastic scintillators is perpendicular to each other. In each layer, 10 scintillators are arranged in a wall of 700×700 mm^2. Signals from the FPS are read out by MPPCs located at both sides of the individual scintillator.

There remains a gap for neutral-particle detection between the BGOegg calorimeter and

the FG, corresponding to the polar angle range of 16–24 degrees. We are planning to cover this region by adding about two layers of BGO crystals in the next step of the Phase-II experiment. This procedure is relatively easy by remaking the cone support that holds the whole egg-shaped assebly from the downstream side. If most of the solid angles are covered by electromagnetic calorimeters, we can explore wider physics possibilities other than the studies of η' mass in nuclei; For example, it becomes possible to investigate higher resonance states that produce multiple π^0 and η.

5 Sensitivity discussions

We are going to use a copper target instead of a carbon target, used in the Phase-I experiment. While the radius of a carbon nucleus is 2.7 fm, that of a copper nucleus increases to 4.8 fm. If η' mesons are produced inside a nucleus that has a larger radius, the probability of decays in the environment with a nuclear density becomes higher. Table 1 shows the estimated ratio of in-medium decays in the $\eta' \to \gamma\gamma$ channel under the assumption that its partial decay rate is unchanged in the nucleus and the outside vacuum. This ratio depends on the requirement to select low-momentum η' mesons. Here we simulated the η' production and decays inside a nucleus by taking into account the Woods-Saxon type density distribution and the density dependence of production and decay rates. Because data statistics become significantly high in the BGOegg Phase-II experiment, we can select the momentum region whose upper boundary is lower than that of the Phase-I experiment. In case of using a copper-nucleus target and selecting the η' momentum less than 600 MeV/c, the ratio of in-medium decays is about 5 times of that in the Phase-I experiment.

Table 1: Estimated ratios of $\eta' \to \gamma\gamma$ decays before η' mesons go out of a nucleus. The estimation was performed depending on the sample selection condition of η' momenta.

Momentum selection	< 400 MeV/c	< 600 MeV/c	< 1000 MeV/c
C target ($r = 2.7$ fm)	0.7%	0.5%	0.2%
Cu target ($r = 4.8$ fm)	1.7%	1.0%	0.4%

Installation of additional forward calorimeters is essential to enhance the statistical significance of η'-mass reduction signals by decreasing multi-meson backgrounds down to a sufficiently low level. Also, a good signal-to-noise ratio is a key to exclude possibilities of mistakenly recognizing the enhancement due to unknown systematic uncertainties as signals. For the case of combining the FG with the BGOegg calorimeter, we estimated a rejection factor against the

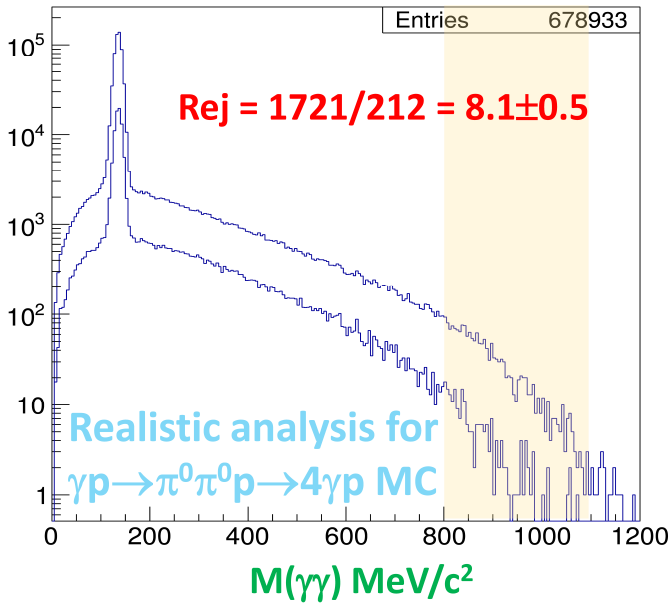

Figure 6: Invariant mass distributions of $\gamma\gamma$ pairs for a realistic Monte-Carlo simulation of the $\gamma p \to \pi^0\pi^0 p \to 4\gamma p$ reaction. Two cases with only the BGOegg calorimeter and both of the BGOegg and the FG are overlayed. A background rejection factor by the installation of FG was estimated in the shaded area.

$\gamma p \to \pi^0\pi^0 p \to 4\gamma p$ reaction, which should be dominant as a background source. This reaction was generated in the Monte-Calro simulation with a realistic experimental setup, and a set of event selection conditions used in the analysis of the Phase-I experiment were required to the generated sample. As shown in Fig. 6, the rejection factor is estimated to be 8.1 ± 0.5, corresponding to the background reduction by about one order of magnitude, in the region near the nominal η' mass. If we expand the forward acceptance of the BGOegg calorimeter by adding new BGO crystals and cover the gap to the FG, the rejection factor will increase up to 40.

In the direct measurement by the Phase-I experiment, the η'-mass reduction inside a carbon nucleus was indicated as a low mass component below the quasi-free η' photoproduction peak. However, its statistical significance was not high enough, and this indication must be confirmed by a new experimental setup that improves data statistics and a signal-to-noise ratio. In the BGOegg Phase-II experiment, we are planning to use a copper target with a thickness of 0.5 radiation lengths and a photon beam whose intensity exceeds 3×10^6 s^{-1}. As discussed in the beginning of this section, the use of copper nuclei will increase the ratio of in-medium

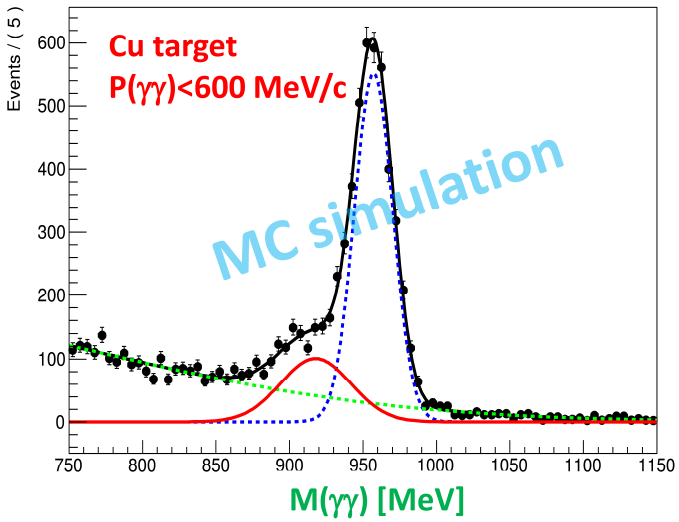

Figure 7: A $\gamma\gamma$ invariant mass spectrum expected in the BGOegg Phase-II experiment with the additional installation of the FG and FPS.

decays 5 times more than that of the Phase-I experiment in the $\gamma\gamma$ momentum region less than 600 MeV/c. At an initial stage of the Phase-II experiment, we will start data collection with the FG and FPS to reduce the multi-meson backgrounds by one order of magnitude. Figure 7 shows a $\gamma\gamma$ invariant mass distiribution, where the signal amount is estimated by taking into account the above key numbers for the Phase-I result. The mean of signal distribution is assumed to be about 920 MeV/c^2 with the sigma of 24 MeV/c^2, as observed in the Phase-I analysis. In the case of Fig. 7, the statistical siginificance of signals reaches 28σ in two-month data taking. In parallel, we proceed with the preparation for the extension of the BGOegg calorimeter for further background suppression in the case that signals are not well observed in the first physics runs of the Phase-II experiment, mentioned above. The second stage of the Phase-II experiment will be separately proposed with updated sensitivity discussions after examining the first-run data.

In the data analysis, we will examine the existence of signal enhancement by several different methods. In one method, the significance of an excess is examined only by fitting background functions without a signal region of the $\gamma\gamma$ invariant mass distribution. This way will provide the information of a possible excess independently of η'-mass reduction models. In another method, we examined the significance of an excess by the χ^2 difference test with and without a signal function of the η'-mass reduction. The signal function will be prepared by taking into account the position dependence of density, η'-production rate, decay width, and mass reduction

inside a copper nucleus. Also, a simple Gaussian function will be fitted as an alternative signal function in a less model-independent way. From these fitting results, we will discuss the amount and width of η'-mass reduction and the in-medium decay rate.

6 Preparation status

The FG was developed for SPring-8 LEPS experiments that was carried out in 2003 by combining it with Backward Gamma detectors [25]. Since the FG was used about 20 years ago, we re-evaluated its performance at the ELPH positron beamline. In particular, we examined the incident-angle dependence of energy resolutions and the position resolution of FG hits because they had not been measured. As a result of the beam test, the energy resolution of 2.7% was obtained for 1 GeV positrons. This value is comparable to the results of previous experiments [26]. In addition, the energy resolution was evaluated by changing the angle of FG from 0 to 16 degrees while keeping the incident position at the center of a certain crystal. Detailed results are reported in ELPH annual report 2018 [28].

After the performance test in ELPH, the FG was transported to the SPring-8 LEPS2 experimental building. It is now located on a movable stage at the downstream of the BGOegg calorimeter. A beam test of the FG with the BGOegg calorimeter and the FPS was performed at the LEPS2 beamline in 2019. We tested only 16 channels of the FG, but successfully confirmed that it was properly working along with the BGOegg DAQ system. The FPS also shows good performance to identify a charged cluster in the FG [27]. Currently, the data acquisition system of the FG is being constructed and integrated to the BGOegg DAQ system. Unfortunately, the BGOegg DAQ system partly based on CAMAC has become old, and some circuit boards are damaged. We need to replace the damaged part to a new system based on VME. The forward expansion of the BGOegg calorimeter is now under consideration and being designed.

In order to increase both the photon beam intensity and the copper target thickness, we need to clear a radiation safety problem. We have estimated a radiation level with a target thiclness of 0.5 radiation lengths and a beam intensity of 5×10^7 s^{-1} over all the energy range, and concluded that a concrete shield around the beam dump must be increased at the LEPS2 experimental building [29]. We are now consulting with the radiation safety office of SPring-8.

7 Other physics possibilities

7.1 $f_1(1285)$ meson photoproduction

We are considering to measure the mass shift and width broadening of the $f_1(1285)$ meson inside a nucleus. The $f_1(1285)$ meson can be a chiral partner of the ω meson, and they may be degenerated when the chiral symmetry is restored. Thus, the photoproduction of $f_1(1285)$ in a nuclear target is a good way to experimentally probe the partial restoration of chiral symmetry inside nuclear matter. The medium modification of the $f_1(1285)$-meson mass is discussed on the basis of the spontaneous breaking of chiral symmetry, and complementary to the in-medium η' mass modification, which must be also related with the $U_A(1)$ quantum anomaly. A QCD sum rule analysis for the $f_1(1285)$-meson mass predicts about 100 MeV attraction at the normal nuclear density [30], and it can be probed in our experiment. We have already observed a peak of the $f_1(1285)$ in the $\pi^0\pi^0\eta$ (6γ) decay mode. The BGOegg calorimeter has achieved a good mass resolution of about 6 MeV by using a kinematical fit with the mass constraints for π^0 and η. This resolution is much better than the full width of 24.2 MeV, and the change of spectral shape is precisely detectable. The Phase-II experiment will reduce multi-meson backgrounds and improve the statistical significance of $f_1(1285)$ signals.

7.2 Photoproduction of η' mesons from nuclei near the production threshold

Another interesting case of the hadron medium effect is the measurement of excitation functions for the photoproduction of η' mesons off nuclei. A recent paper [31] reported the calculation of in-medium mass shift on the basis of an approach that takes into account both primary photon-nucleon and secondary pion-nucleon η' production processes as well as two different scenarios with and without the in-medium η' mass shift. In this calculation, one can see well-separated predictions for these two scenarios, so that the excitation function for η' photoproduction off nuclei are appreciably sensitive to the η'-mass shift. Because the BGOegg experiment well covers the threshold energy region, the Phase-II experiment gives an opportunity to measure the excitation function for η' photoproduction from nuclei with increased statistics compared with the Phase-I. This measurement will be useful to help determine a possible η' mass shift in nuclear matter.

7.3 Photon beam asymmetry of the η' photoproduction on the proton

We are considering to measure the photon beam asymmetry of the η' meson from a proton target in the energy range $1.9 < W < 2.3$ GeV. The CLAS collaboration reported the photon beam asymmetry results for $\gamma p \to \eta' p$ reaction in an energy range $1.9 < W < 2.1$ GeV [32], and a theoretical analysis was done [33]. In this analysis, it was concluded that a satisfactory description of the available data on both differential cross sections and photon beam asymmetries can be obtained by including in the s-channel three-star resonance $N(1875)3/2$- and one-star resonance $N(2040)3/2+$. The resonance $N(1875)3/2$- contributes significantly in the energy range from the threshold up to $W \sim 2.3$ GeV and the resonance $N(2040)3/2+$ provides smaller but considerable contributions in the energy range of $2.0 < W < 2.3$ GeV in differential cross sections. A similar trend of these contributions is seen in photon beam asymmetry, but experimental data has covered only $W < 2.1$ GeV. The BGOegg experiment covers $W < 2.3$ GeV with a highly linear-polarized photon beam and provides precise data of photon beam asymmetries in high energy regions. In the Phase-I experiment, we have already measured η' photoproduction reaction but the statistics of η' signals is not enough. The Phase-II experiment can provide the η' signals more efficiently by improving acceptance and beam intensity.

7.4 $\pi^0\pi^0$ momentum correlations

We plan to measure the spatial extent of intermediate baryon resonances and of hadron reaction volume in the non-perturbative QCD energy region to have better understanding of hadron structure and strong interaction. It is difficult, however, to measure the size of unstable hadron resonances due to their short lifetime. We here propose a new method to measure the spatial extent of the $\Delta(1232)$ resonance involved in the sequential decay process $\gamma p \to \pi^0 \Delta^+ \to \pi^0 \pi^0 p$, where an energetic quark emerges in the proton by the incident photon, subsequently producing a π^0 and forming a Δ. The first emitted π^0 originates from the energetic quark, the spin of which flips at the same time so as to form the Δ after π^0 emission. It may be natural to think that the wave functions of π^0 and Δ overlap with each other at the origin of the $\pi^0\Delta$ system. Thus we assume that the first π^0 appears somewhere within Δ according to the quark distribution and then goes apart from the Δ, which sequentially emits the second π^0 afterward. Under this assumption, the Bose-Einstein correlation of these two π^0's may give information on the size of Δ.

The electromagnetic calorimeter BGOegg enables an unprecedented high-resolution measurement, providing precise data for $\pi^0\pi^0$ relative momenta. Nearly 4π coverage by the BGOegg calorimeter opens the possibility of $\pi^0\pi^0$ correlation measurements, which have not been done in the non-perturbative energy region. In the photon-beam energy region of 1.3–2.4 GeV, s-channel resonance contributions coupling to $\pi^0\pi^0 p$ are weak, and it becomes possible to select a clean sample for examining $\pi^0\pi^0$ correlations. Therefore, we will investigate the double neutral pion photoproduction $\gamma p \to \pi^0\pi^0 p$ and analyze the correlation effects of $\pi^0\pi^0$ to obtain information about the size of a specific intermediate resonance like $\Delta(1232)$.

7.5 Subjects under considerations

We would also like to investigate highly excited baryon resonances by measuring two mesons that are photoproduced from a proton target. (See Refs. [34] and [35] as examples.) Since the highly excited baryons do not strongly couple to the $N\pi$ channel, properties of only few high-mass baryons have been well established. Double-meson photoprodution experiments are desired to clarify the existence of high-mass baryons and extract their properties. Different combinations of two produced mesons put restrictions for the excited high-mass baryons that can appear as an intermediate state. A wide angular corverage of the particle detection is desirable for the resonance search through double-meson production, as being done in the BGOegg Phase-II experiment.

We are considering to study the nature of tensor force in a nucleus by measuring the short-range correlation between two nucleons. Tensor force has a strong selection mechanism for neutron-proton (np) pairs [36]. The short range correlated effect will be accessible by measuring the cross-section ratio of correlated pp and np pairs with the variation of relative momentum up to 3 fm^{-1}.

8 Experimental group

The BGOegg experiment is carried out by an international collaboration led by ELPH, Tohoku University. In addition to the Phase-I collaboration, new members from China has joined to the new project. The LEPS2 beamline is co-operated by RCNP, Osaka University and ELPH, Tohoku University.

- Research Center for Electron Photon Science (ELPH), Tohoku University : N. Muramatsu, M. Miyabe, T. Ishikawa, Y. Matsumura, H. Ohnishi, M. Okabe, Y. Sada, H. Shimizu, A. O. Tokiyasu, M. Tsuruta, C. Yoshida

- Research Center for Nuclear Physics (RCNP), Osaka University : S. Daté, T. Hashimoto, T. Hotta, H. Katsuragawa, T. Nakano, T. Nam, Y. Ohashi, S.Y. Ryu, S. Tanaka, N. Tomida, T. Yorita, M. Yosoi
- Department of Physics, Korea University : J.K. Ahn
- Institute of Physics, Academia Sinica : W.C. Chang
- National Synchrotron Radiation Research Center : J.Y. Chen
- Department of Nuclear Science & Engineering, College of Material Science and Technology, Nanjing University of Aeronautics and Astronautics : Q.H. He, S.K. Wang
- Department of Physics and Astronomy, Ohio University : K. Hicks
- Department of Physics, Kyoto Sangyo University : M. Niiyama
- Department of Physics and Engineering Physics, University of Saskatchewan : C. Rangacharyulu
- Laboratory of High Energy Physics, Joint Institute for Nuclear Research: E. A. Strokovsky
- Department of Education, Gifu University : M. Sumihama
- Japan Synchrotron Radiation Research Institute (SPring-8) : S. Suzuki
- School of Physics, Beihang University : T.F. Wang

9 Beamtime request and expected schedule

Beamtime request: We request two-month test-experiment with a Copper target of 0.1 radiation lengths in FY2022 and four-month physics data collection with 0.5 radiation lengths in FY2023. We need additional four-month experiment with a liquid hydrogen (LH_2) target to collect reference data.

This research will be supported in part by KAKENHI, Grant-in-Aid for Scientific Research (S), 21H04986. We will first finalize the setup with the FG and FPS in addition with the repairment of the BGOegg DAQ system. A photon beam intensity will be also increased soon by introducing another pulsed laser. After these minimum preparation, test-data collection will be done initially with a copper target whose thickness is kept at 0.1 radiation lengths (X_0) in FY2022. In parallel, we plan to proceed with the application of radiation safety change to use

a $0.5X_0$ target and construct an additional concrete wall around the beam dump. In FY2023, we will collect high-statistics physics data for a half year with a $0.5X_0$ copper target and other upgrades mentioned above to search for the η' mass reduction inside a nucleus (first runs). We will also collect reference data with a LH_2 target for a half year in FY2023 or 2024. The liquid target system must be shared with the LEPS2/Solenoid experiment. In FY2022 and 2023, we will prepare for the forward expansion of the BGOegg calorimeter by designing, producing, wrapping, and testing new crystals. The new crystals will be assembled after the first runs of the Phase-II experiment. We will update the discussions of a signal sensitivity for the next proposal. We are considering to promote the BGOegg Phase-II experiment as follows:

2022	Apr.	Start the preparation of the FG and FPS readout system.
		Start the works to repair the BGOegg DAQ system.
	June	Application of radiation shielding change around the beam dump.
	Aug.	Introduction of an additional pulsed laser system.
	Nov.	Test data-taking with a $0.1X_0$ copper target.
	Dec.	Strengthenning a concrete shield at the beam dump
		to make a copper target thicker to $0.5X_0$.
2023	Oct.	Start of the first physics runs of the Phase-II experiment
		with a $0.5X_0$ copper target. (Need negotiation with the Solenoid
		experiment for alternative operation.)
2024	Apr.	Collection of the reference data with a LH_2 target.
	Aug.	Forward expansion of the BGOegg calorimeter.
		(The preparation will be done in FY2022–2023.)

References

[1] E. Witten, Nucl. Phys. B 156 (1979) 269.

[2] G. Veneziano, Nucl. Phys. B 159 (1979)

[3] S.H. Lee and T. Hatsuda, Phys. Rev. D 54 (1996).

[4] S. Kono, D. Jido, Y. Kuroda, and M. Harada, Prog. Theor. Exp. Phys. 2021-9 (2021) 093D02.

[5] H. Nagahiro. M. Takizawa, and S. Hirenzaki, Phys. Rev. C 74 (2006) 045203.

[6] S. Sakai and D. Jido, Phys. Rev. C 88 (2013) 064906.

[7] S.D. Bass and A.W. Thomas, Phys. Lett. B 634 (2006) 368.

[8] E. Czerwinski et al., Phys. Rev. Lett. 113 (2014) 062004.

[9] M. Nanova, V. Metag, A. Ramos, E. Oset, I. Jaegle, K. Makonyi, et al. (CBELSA/TAPS Collaboration), Phys. Lett. B 710 (2012) 600.

[10] M. Nanova, V. Metag, E.Ya. Paryev, et al. (CBELSA/TAPS Collaboration), Phys. Lett. B 727 (2013) 417.

[11] M. Nanova, S. Friedrich, V. Metag, E.Ya. Paryev, et al. (CBELSA/TAPS Collaboration), Phys. Rev. C 94 (2016) 025205.

[12] S. Friedrich, M. Nanova, V. Metag, et al. (CBELSA/TAPS Collaboration), Eur. Phys. J. A 52 (2016) 297.

[13] M. Nanova, S. Friedrich, V. Metag, E.Ya. Paryev, et al. (CBELSA/TAPS Collaboration), Eur. Phys. J. A 54 (2018) 182.

[14] Y.K. Tanaka, K. Itahashi, H. Fujioka, et al. (η-PRiME/Super-FRS Collaboration), Phys. Rev. Lett. 117 (2016) 202501.

[15] Y.K. Tanaka, K. Itahashi, H. Fujioka, et al. (η-PRiME/Super-FRS Collaboration), Phys. Rev. C 97 (2018) 015202.

[16] N. Tomida, N. Muramatsu, M. Niiyama, et al. (BGOegg Collaboration), Phys. Rev. Lett. 124 (2020) 202501.

[17] Y. Matsumura, Doctoral Thesis (Tohoku Univ.), 2021.

[18] H. Nagahiro, JPS Conf. Proc. 13 (2017) 010010.

[19] N. Muramatsu, M. Yosoi, T. Yorita, Y. Ohashi, et al., arXiv:2112.07832 (2021).

[20] N. Muramatsu, Y. Kon, S. Daté, Y. Ohashi, et al.., Nucl. Instrum. Methods A 737 (2014) 184; N. Muramatsu, M. Yosoi, T. Yorita, and S. Suzuki, J. Particle Accelerator Society of Japan, Vol. 10, No. 3 (2013) 171.

[21] N. Muramatsu, arXiv:1307.6411 (2013); ELPH Report 2044-13 (2013).

[22] H. Katsuragawa, RCNP Annual Report 2020, Osaka Univ. (2021) “Highlights” section.

[23] T. Ishikawa, et al., Nucl. Instrum. Methods A 837 (2016) 109.

[24] T. Nam, Doctoral Thesis (Osaka Univ.), 2019; N. Muramatsu, et al. (LEPS2/BGOegg Collaboration), Phys. Rev. C 100 (2019) 055202; N. Muramatsu, et al. (LEPS2/BGOegg Collaboration), Phys. Rev. C 102 (2020) 025201.

[25] T. Ishikawa et al., Nucl. Instrum. Meth. A 832, (2016) 108.

[26] H. Shimizu et al., Nucl. Instrum. Meth. A 447 (2000) 467.

[27] T. Ueda, Master Thesis (Tohoku Univ.), 2018.

[28] M. Miyabe et al., ELPH annual report 2018 (2019) 22.

[29] Y. Asano, private communications.

[30] P. Gubler, T. Kunihiro, S.H. Lee, Phys. Lett. B 767 (2017) 336.

[31] E Ya Paryev, J. Phys. G: Nucl. Part. Phys. 40 (2013) 025201.

[32] P. Collins et al., Phys. Lett. B 771 (2017) 213.

[33] Y. Zhang, A.C. Wang, N.C. Wei, and F. Huang, Phys. Rev. D 103 (2021) 094036.

[34] Y. Assafiri et al., Phys. Rev. Lett. 90 (2003) 222001.

[35] V. Sokhoyan et al., Eur. Phys. J. A 51 (2015) 95.

[36] R. Schiavilla et al., Phys. Rev. Lett. 98 (2007) 132501.